December 2001 • NREL/SR-520-31379

Subcontractor Report

Transparent Conductors and Barrier Layers for Thin Film Solar Cells

Final Technical Report
15 June 2001

R.G. Gordon, R. Broomhall-Dillard, X. Liu, D. Pang, and J. Barton
Harvard University
Cambridge, Massachusetts

National Renewable Energy Laboratory

1617 Cole Boulevard
Golden, Colorado 80401-3393

NREL is a U.S. Department of Energy Laboratory
Operated by Midwest Research Institute • Battelle • Bechtel

Contract No. DE-AC36-99-GO10337

December 2001 • NREL/SR-520-31379

Transparent Conductors and Barrier Layers for Thin Film Solar Cells

Final Technical Report
15 June 2001

R.G. Gordon, R. Broomhall-Dillard, X. Liu, D. Pang, and J. Barton
Harvard University
Cambridge, Massachusetts

NREL Technical Monitor: B. von Roedern

Prepared under Subcontract No. XAK-8-17619-26

National Renewable Energy Laboratory

1617 Cole Boulevard
Golden, Colorado 80401-3393

NREL is a U.S. Department of Energy Laboratory
Operated by Midwest Research Institute • Battelle • Bechtel

Contract No. DE-AC36-99-GO10337

NOTICE

Available electronically at http://www.doe.gov/bridge

Available for a processing fee to U.S. Department of Energy
and its contractors, in paper, from:

U.S. Department of Energy
Office of Scientific and Technical Information
P.O. Box 62
Oak Ridge, TN 37831-0062
phone: 865.576.8401
fax: 865.576.5728
email: reports@adonis.osti.gov

Available for sale to the public, in paper, from:

U.S. Department of Commerce
National Technical Information Service
5285 Port Royal Road
Springfield, VA 22161
phone: 800.553.6847
fax: 703.605.6900
email: orders@ntis.fedworld.gov
online ordering: http://www.ntis.gov/ordering.htm

Printed on paper containing at least 50% wastepaper, including 20% postconsumer waste

Contents

List of Figures

List of Tables

Executive Summary

Task 1: CVD of Zinc Stannate Films and Other Buffer Layers

Amorphous silicon solar cells based on fluorine-doped zinc oxide superstrates have demonstrated currents about 10% larger than similar cells on commonly-used fluorine-doped tin oxide. However, lower fill factors had previously negated this advantage of zinc oxide. Three different buffer layers were placed between the zinc oxide and the amorphous silicon in efforts to improve the fill factors:

1) A new CVD process was developed for making zinc stannate films with various ratios of zinc to tin. While the fill factors were improved over those of zinc oxide, they still fell short of those for standard tin oxide by a few per cent.
2) Niobium-doped titanium dioxide is highly resistant to reduction by hydrogen plasma. However, its fill factors were even lower that those without this buffer layer.
3) Cells with efficiency 10% higher than standard tin oxide were finally achieved by a proprietary buffer layer developed at BP Solar, while maintaining equal fill factors.

Task 2: CVD of Fluorine-doped Zinc Oxide Films

The CVD of highly transparent ZnO:F films was developed to provide better control of the surface roughness and the resulting haze and light trapping. Haze values of only 4% yielded optimal light trapping, with currents up to 10% higher than standard tin oxide. Variations on the growth conditions for a-Si, such as microcrystalline p-layers and hydrogen plasma pretreatments, did not produce the consistently high fill factors made with BP Solar's buffer layer.
Larger than usual numbers of shunted cells were found among the cells made on ZnO:F. Reduction of these shunts remains a problem to be solved.

Task 3: CVD of Aluminum Oxide Films

Aluminum oxide-coated glass plates are used as substrates for deposition of fluorine-doped zinc oxide for three different reasons.

1) Use of an alumina layer between soda-lime glass and fluorine-doped zinc oxide films was found to provide a 10% reduction in their sheet resistance. Alumina is an outstanding barrier to diffusion of sodium. Thus it prevents contamination of the film by sodium, which traps and scatters the conduction electrons in the zinc oxide films.
2) Nucleation of fluorine-doped zinc oxide appears to be more uniform and consistent on alumina surfaces than on bare glass substrates. Thus it provides better control of roughness and the resultant haze that is needed for efficient light-trapping in amorphous silicon solar cells.
3) The transmission of light through the films is increased by a per cent or so because alumina has a refractive index intermediate between that of glass and zinc oxide.

Two different liquid precursors were investigated for the CVD of alumina films: triethyldialuminum tri-*sec*-butoxide[1] and mixed aluminum betadiketonates.[2] Both of these precursors are now commercially available from Strem Chemical Company. Both precursors were used successfully to make amorphous aluminum oxide films used in this project.

Background, Approaches Taken and Summary of Results

This research was undertaken to increase the efficiency of thin-film solar cells based on amorphous silicon in the so-called superstrate structure (glass front surface/transparent electrically conductive oxide (TCO)/pin amorphous silicon/metal back electrode). The TCO layer has to meet many requirements: high optical transparency in the wavelength region from about 350 nm to 900 nm, low electrical sheet resistance, stability during handling and deposition of the subsequent layers and during use, a textured (rough) surface to enhance optical absorption of red and near-infrared light, and low-resistance electrical contact to the amorphous silicon p-layer. Fluorine-doped tin oxide[3] has been the TCO used in most commercial superstrate amorphous silicon cells.

Fluorine-doped zinc oxide (ZnO:F) was later shown to be even more transparent than fluorine-doped tin oxide,[4] as well as being more resistant to the strongly reducing conditions encountered during the deposition of amorphous silicon.[5] Solar cells based on ZnO:F showed the expected higher currents, but the fill factors were lower than standard cells grown on tin oxide, resulting in no consistent improvement in efficiency. This problem was attributed to a higher electrical resistance between ZnO:F and silicon.[6]

One approach to decreasing the electrical resistance between ZnO:F and silicon was to insert a buffer layer between them. It seemed possible that a zinc stannate composition might combine the best features of zinc oxide's stability with tin oxide's ability to form a low resistance contact to silicon.[7] Under **Task 1** of this contract, a process was developed for the chemical vapor deposition (CVD) of zinc stannate with various zinc/tin ratios, and solar cells were grown on these layers. Another buffer layer that was investigated was titanium oxide, since it is also high resistant to reduction by hydrogen plasmas. Other proprietary buffer layers made at BP Solar were also investigated, leading finally to a buffer layer that succeeded in producing low resistance contact between silicon and ZnO:F, and cells with 10% higher efficiency than standard cells on tin oxide.

Another approach to reducing the contact resistance to ZnO:F was to modify the surfaces in contact. In **Task 2**, several such surface modifications were explored. Wet etching of the zinc oxide surface showed some promising results in reducing the contact resistance (perhaps by providing a clean surface), but the results were not reproducible. The wet etching also provides a ready means for controllably increasing the surface roughness to any desired level, to optimize the light-trapping. Previous work had indicated that microcrystalline p-layers could be deposited on ZnO without reduction, so solar cells with various microcystalline p-layers were made. Optimization of the p-layers did not, however, improve the efficiency of ZnO:F cells beyond those made on tin oxide.

The optical and electrical performance of TCO layers have been known to be adversely affected by diffusion of sodium from soda-lime glass substrates during the deposition of the TCO. Silicon dioxide is the barrier material most commonly used between tin oxide and glass. In **Task 3**, barriers to diffusion of sodium were investigated. CVD layers of aluminum oxide were found to be far better barriers to the diffusion of sodium. The sheet resistances of ZnO:F films were reduced by about 10% by putting an aluminum oxide film between ZnO:F and glass substrates.

Task 1: CVD of Zinc Stannate Films and Other Buffer Layers

Films of zinc stannate were deposited by CVD at atmospheric pressure from a solution of the precursors dibutyltin diacetylacetonate, $Bu_2Sn(acac)_2$, and zinc acetylacetonate, $Zn(acac)_2$ in di(ethylene glycol)methyl ether, $CH_3OCH_2CH_2OCH_2CH_2OH$. The reactant gas mixture was prepared by placing such a solution in a syringe pump from which it was delivered at a steady rate of 3 – 15 ml/hr into a Sonotek ultrasonic nozzle operated with 2.0 watts of power at 125 kHz. The resulting fog was entrained into a 5-10 L/min nitrogen gas stream preheated to 220-240 ^oC in order to vaporize the liquid droplets. The resulting gas mixture was then mixed in a T joint with a 0.25-1.5 L/min stream of preheated oxygen gas (also 220-240 ^oC) before reaching the inlet to the reactor. The substrates rested on a nickel plate that was electrically heated from below. The reactant gas mixture flowed over the substrate in a rectangular channel defined by another nickel plate held 1 cm above the substrate by thin nickel alloy (Hastelloy C) spacers that defined the sides of the gas flow channel. The substrate temperature was held at 400-550 ^oC, while the top nickel plate was at 200-250 ^oC. Nearly infinite variability of Zn:Sn stoichiometry in the films was obtained by adjusting the relative precursor concentrations in solution and the deposition parameters (e.g. O_2 flow rate, substrate temperature). All as-deposited films were amorphous by x-ray diffraction analysis (XRD). A typical spectrum is shown in Figure 1:

Figure 1: Diffractogram for Amorphous Zinc Stannate

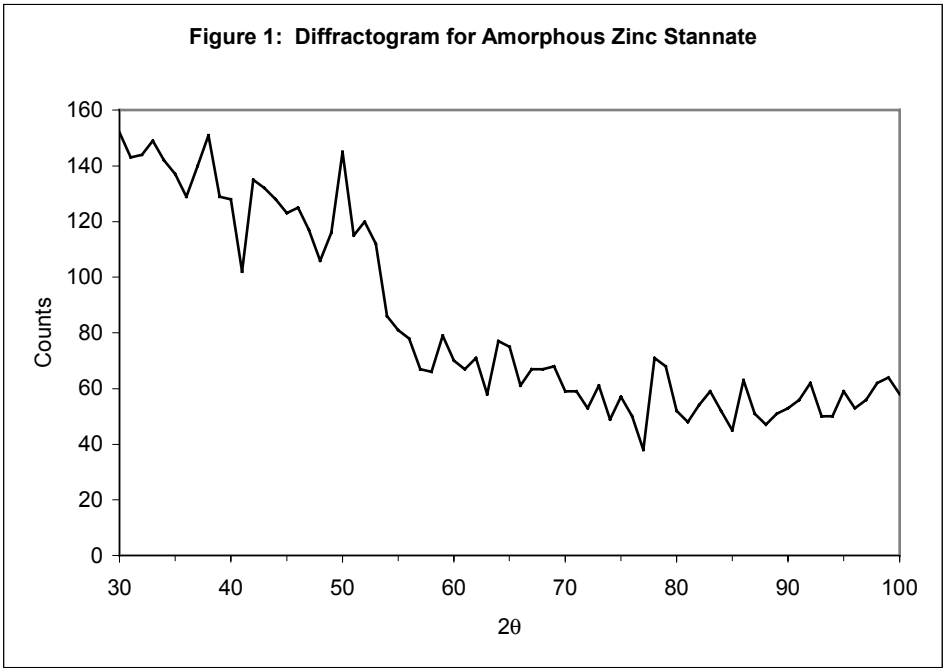

By annealing films of different compositions at 500 ^oC in air for several hours, two different crystalline phases were observed by XRD – one of $ZnSnO_3$, obtained by annealing a low-zinc content film, and one of spinel Zn_2SnO_4, obtained from a high-zinc content film. Annealing in air also served to remove any carbon impurity detectable by Rutherford backscattering (RBS).

A "zinc-rich" film was obtained using a 2:1 Zn:Sn molar ratio precursor solution, using conditions described below. The simulation of the RBS spectrum shown in Figure 2 was for a 2800 Å film of composition $Zn_{1.44}SnO_{3.89}$.

Figure 2: RBS Spectrum and Simulation of Zinc-Rich Film

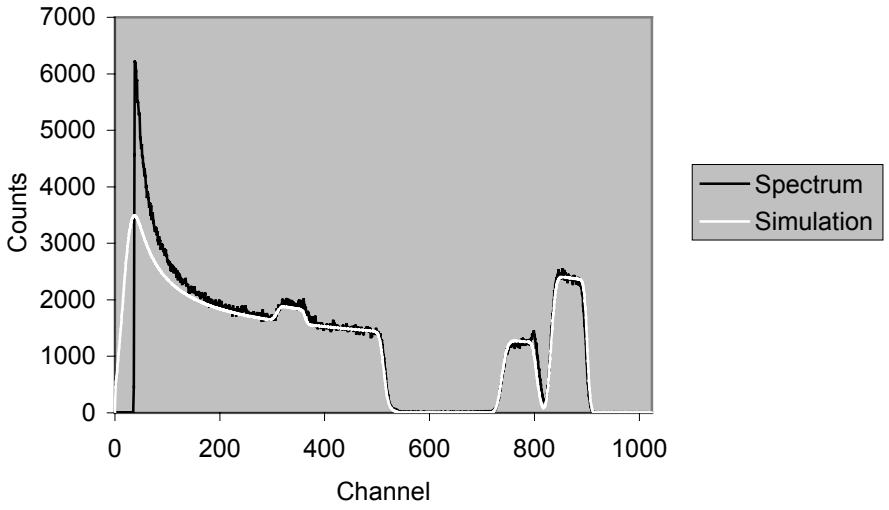

A thicker film was deposited using identical conditions, only 3.5 mL of precursor instead of 0.6mL. This film was annealed at 500 ^{o}C in air for 14.3h. A spinel-type Zn_2SnO_4 phase[8] was subsequently detected by XRD, as shown in Figure 3:

Figure 3: Diffractogram for Zn_2SnO_4 Phase

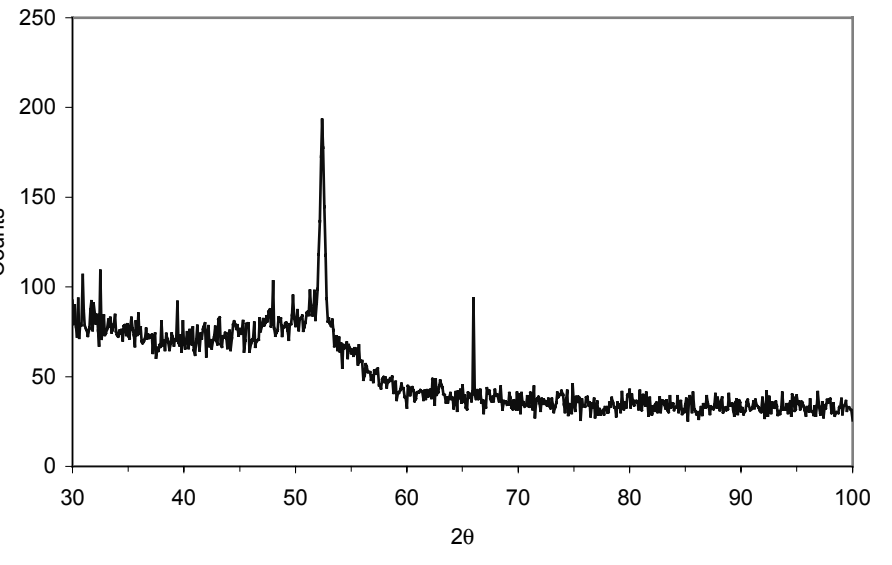

A "tin-rich" film was deposited using 1:1 Zn:Sn molar ratio precursor solution, using conditions described below. A simulation of the RBS spectrum shown in Figure 4 found it to be a 3950 Å film of composition $ZnSn_{3.13}C_{2.66}O_{8.75}$.

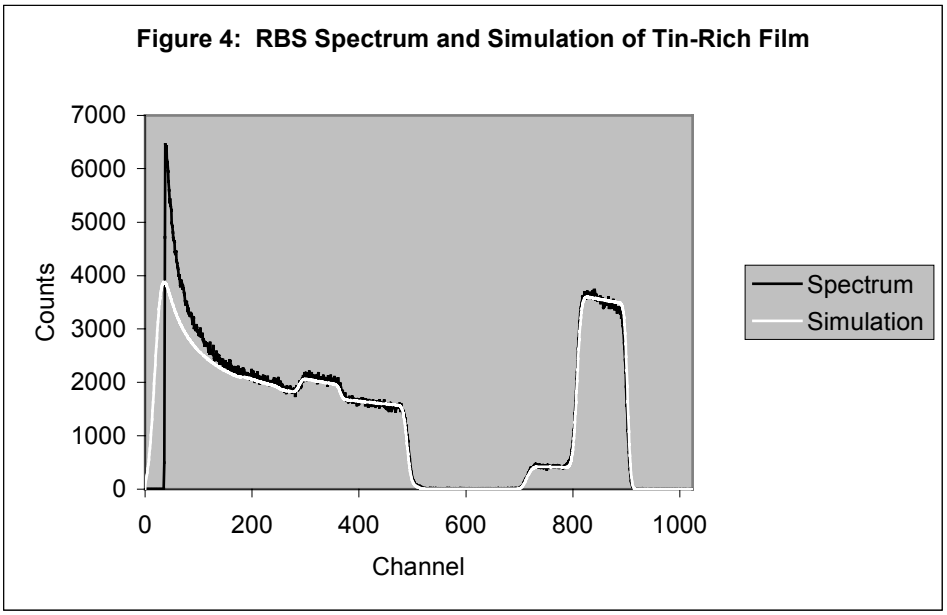

A thicker film was deposited using similar conditions, only using 2.5 mL of precursor instead of 0.74 mL. This film was annealed at 500 ^{o}C in air for 4h. Subsequent XRD analysis (Figure 5) revealed three peaks, which correspond to a previously reported[9] $ZnSnO_3$ phase.

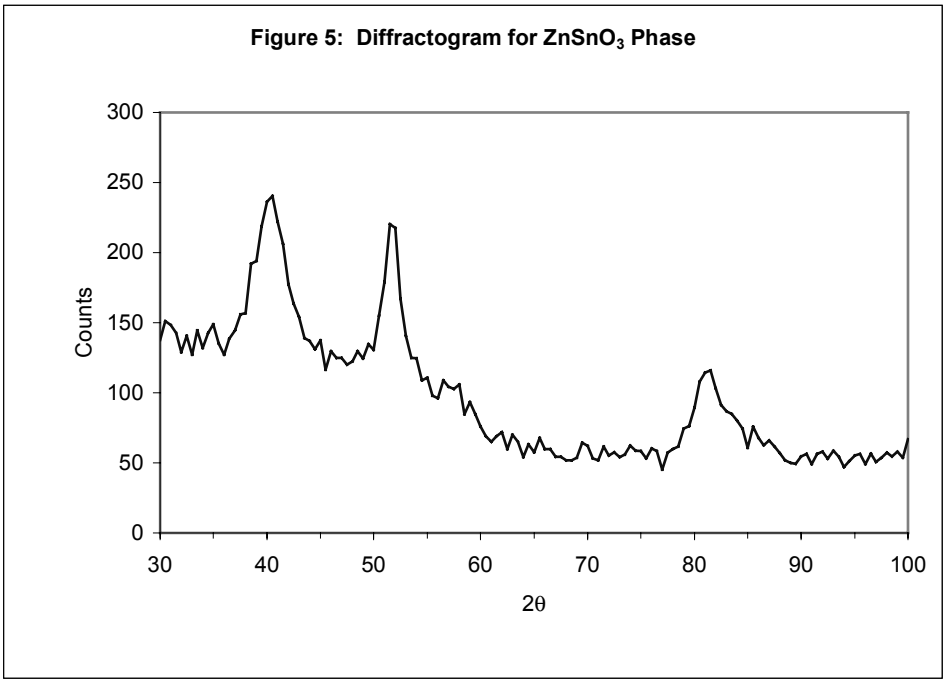

Rutherford backscattering spectra (RBS) were taken for a number of zinc stannate films in order to verify their composition. The ratio of zinc to tin was found to increase as the gas flowed over the substrate. In other words, the tin precursor is more reactive and preferentially deposits tin

closer to the gas inlet, while the zinc precursor is less reactive and deposits more efficiently further along in the gas flow.

Figure 6. Zn/Sn Ratio for CVD Zinc Stannate Films Deposited from $Zn(acac)_2$ and $Me_2Sn(\beta\text{-diketonates})_2$.

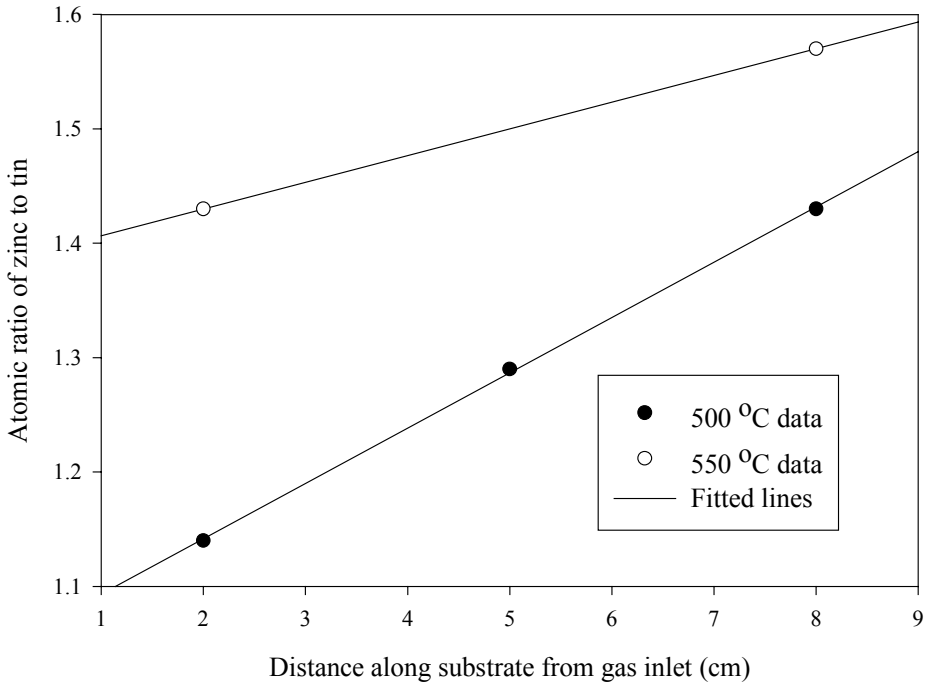

This variation in composition makes it difficult to deposit zinc stannate films with homogeneous and uniform compositions using the present precursors and oxidizing deposition conditions. A less reactive tin precursor and/or a more reactive zinc precursor would be helpful in CVD of zinc stannate films with more uniform composition.

Zinc stannate films were eventually prepared with fairly uniform composition, low carbon content and low visible absorption. The best strategy that we have found for simultaneously achieving these properties is to deposit films at substrate temperatures around 400 ^{o}C with a carrier gas of pure nitrogen and no oxygen. These films have fairly uniform metal content, but high carbon content and high optical absorption. The films are then annealed at 400 ^{o}C in air to remove the carbon and eliminate the optical absorption.

This strategy was applied to make thin films of zinc stannate (100 to 400 Angstroms) as high-resistivity (>100 ohm-cm) buffer layers over highly conductive ZnO:F/glass superstrates. These composite transparent conductors had sheet resistances between 5 and 10 ohms per square, and very small optical absorption (2-3 per cent).

These multilayer transparent conductors were sent to BP Solar, where *pin* amorphous silicon layers and back contacts were deposited. Control samples of fluorine-doped tin oxide (commercial from AFG) were included in each run. The results of 6 different runs showed that nearly the same average efficiencies and open circuit voltages were obtained with the zinc stannate/ZnO:F and the control tin oxide. The zinc stannate/ZnO:F cells showed 3% higher currents than the standard tin oxide, as was expected from the fact that they had higher transparency than the tin oxide. On the other hand, the fill factors of the zinc stannate/ZnO:F cells averaged 3% lower than the tin oxide cells. Detailed results are shown in Table 1.

Table 1. Solar cell parameters for tandem solar cells deposited on zinc stannate/ZnO:F substrates, compared with cells made on commercial (AFG) SnO_2:F in the same run.

Run	Superstrate Sample	FF	Voc	Rs	Rsh	Jsc1	Jsc2	Jsc	Eff.
1	ZnSnOx	0.607	1.469	15.77	2710	8.49	8.32	8.41	7.49
	SnO_2:F	0.653	1.477	15.58	4920	8.11	7.38	7.75	7.47
2	ZnSnOx	0.608	1.464	16.35	3240	8.56	8.28	8.42	7.49
	SnO_2:F	0.657	1.481	15.68	5130	8.13	7.27	7.70	7.49
3	ZnSnOx	0.653	1.493	14.85	3500	8.66	8.88	8.77	8.55
	SnO_2:F	0.666	1.466	15.50	4390	8.30	7.98	8.14	7.95
4	ZnSnOx	0.691	1.500	15.08	4820	8.43	8.03	8.23	8.53
	SnO_2:F	0.703	1.478	15.51	4720	8.28	7.47	7.88	8.18
5	ZnSnOx	0.698	1.499	16.14	5770	8.06	7.13	7.60	7.95
	SnO_2:F	0.703	1.464	13.75	4620	8.27	7.24	7.76	7.98
6	ZnSnOx	0.706	1.498	15.85	5690	7.66	6.85	7.26	7.67
	SnO_2:F	0.721	1.489	15.36	6740	8.24	7.54	7.89	8.47
Average	**ZnSnOx**	**0.661**	**1.487**	**15.67**	**4290**	**8.31**	**7.92**	**8.12**	**7.95**
	SnO_2:F	**0.684**	**1.476**	**15.23**	**5090**	**8.22**	**7.48**	**7.85**	**7.92**

We conclude that zinc stannate buffer layers do not solve the persistent problem of low fill factors shown by ZnO:F in amorphous silicon solar cells.

Additional samples of zinc stannate films with high resistivity and high transparency have been deposited on fluorine-doped tin oxide films. These bilayer TCOs have been supplied to Prof. Chris Ferekides at U. of South Florida and Dr. Gary Dorr at First Solar, for use as superstrates for CdTe solar cells with potentially thinner CdS layers.

Another type of high-resistivity transparent conductor was made from niobium-doped titanium oxide. This material has a higher work function than zinc oxide, and thus it is hoped that TiO_2:Nb could serve as a suitable layer between ZnO:F and the p-layer of an amorphous silicon solar cell. Samples of the structure /TiO_2:Nb/ZnO:F/glass/ were sent to BP Solar for use as superstrates for a-Si solar cells.

Table 2. Single-junction a-Si solar cells grown on composite superstrates with structure/ TiO_2:Nb/ZnO:F/glass/.

Run	Special Condition	Sample	FF	Voc	Rs	Rsh	Jsc	QE @440	QE @500	QE@ @700	Eff.	Shunt %
1	H_2 plasma clean	TiO_2:Nb	0.469	0.792	44.35	759	12.67	602	705	245	4.71	n/a
		SnO_2:F	0.634	0.850	18.91	1430	11.93	566	685	216	6.43	n/a
2	µc-p + a-p	TiO_2:Nb	0.591	0.874	12.80	696	13.18	576	697	313	6.81	58
		SnO_2:F	0.705	0.895	5.69	1140	11.71	532	657	243	7.39	25
3	H_2 plasma + µc-p	TiO_2:Nb	0.505	0.872	15.32	288	9.87	334	499	285	4.35	72
		SnO_2:F	0.656	0.879	6.54	641	9.04	395	485	173	5.21	36

The results, in Table 1, of three runs growing single-junction a-Si solar cells on these superstrates show lower efficiencies than companion cells grown on standard SnO_2:F. Although the currents were higher for the TiO_2:Nb/ZnO:F samples, the fill factors and shunt resistances were much lower than standard cells. With the standard amorphous p-layer, the voltage was also lower. Use of a microcrystalline p-layer restores the voltage, but the efficiency is still lower than for the standard cells. We conclude that the use of TiO_2:Nb as a high-resistance buffer layer on top of a TCO is not a promising approach, even though the material has good resistance to hydrogen plasma.

A third buffer layer was developed at BP Solar. It was deposited on the ZnO:F superstrates before deposition of the amorphous silicon solar cells. Solar cell parameters for some of these cells are given in tabular form in Table 3, and for others in graphical form in Figure 7. The results labeled "new" in Figure 7 include buffer layers on the ZnO:F, while the "standard" process omits the buffer layer on the ZnO:F. The ZnO:F cells with the new buffer layer show an average of 10% higher efficiency and short-circuit current (Jsc) than standard SnO_2:F cells. The quantum efficiencies for blue light (440 nm and 500 nm) are consistently higher on ZnO:F than on SnO_2:F. The quantum efficiencies for red light (700 nm) are only slightly improved, because most of these ZnO:F samples were smoother (lower than 4% haze) than is optimum for light trapping. At the same time, the new buffer layer preserves other parameters at values unchanged from standard SnO_2:F cells: fill factors (FF), open circuit voltages (Voc), series resistances (Rs) and shunt resistances (Rsh).

Each of these runs included 36 solar cells made on the same 3" by 3" superstrate of transparent conductor. The number of shunted cells is still higher for cells on ZnO:F than on SnO_2:F. This difficulty is not improved significantly by the presence of the buffer layer.

Table 3. Solar cell parameters for cells made on fluorine-doped zinc oxide covered by a proprietary buffer layer developed by BP Solar, compared with cells made on commercial (AFG) SnO_2:F. The groups of 2 or 4 results are for cells made side-by-side in the same run.

Subst	FF	Voc	Rs	Rsh	Jsc	QE@	QE@	QE@	Eff	Shunts
		volt	ohm	ohm	ma/cm^2	440nm	500nm	700nm	%	out of 36
ZnO:F	0.723	0.875	5.55	2680	13.07	0.612	0.725	0.319	8.27	5
SnO_2:F	0.714	0.872	6.92	2760	11.59	0.551	0.680	0.225	7.22	3
ZnO:F	0.733	0.876	5.89	2560	12.80	0.600	0.743	0.266	8.22	22
SnO_2:F	0.732	0.877	5.60	2590	11.60	0.536	0.670	0.251	7.45	5
ZnO:F	0.741	0.882	5.43	2680	12.87	0.580	0.709	0.308	8.41	11
SnO_2:F	0.733	0.881	5.45	2370	12.22	0.551	0.687	0.286	7.89	5
ZnO:F	0.709	0.897	7.29	2620	13.02	0.632	0.734	0.270	8.28	15
SnO_2:F	0.737	0.894	5.45	2670	11.87	0.567	0.696	0.229	7.82	8
ZnO:F	0.699	0.876	7.11	2320	13.16	0.612	0.739	0.316	8.06	26
SnO_2:F	0.744	0.882	5.22	2770	11.26	0.530	0.664	0.214	7.39	23
ZnO:F	0.736	0.864	5.58	2910	12.64	0.628	0.742	0.250	8.04	28
SnO_2:F	0.746	0.880	5.29	2670	10.83	0.506	0.637	0.200	7.11	13
ZnO:F	0.746	0.897	5.57	3350	12.21	0.596	0.697	0.181	8.17	18
SnO_2:F	0.750	0.887	5.39	3050	11.83	0.554	0.687	0.221	7.87	2
ZnO:F	0.738	0.904	5.92	3210	12.61	0.597	0.724	0.194	8.41	18
SnO_2:F	0.745	0.894	5.54	3060	11.83	0.560	0.695	0.203	7.88	4
ZnO:F	0.737	0.893	5.55	2810	12.68	0.582	0.704	0.194	8.35	17
ZnO:F	0.734	0.894	5.71	2620	12.69	0.616	0.743	0.177	8.33	24
ZnO:F	0.733	0.873	4.86	1970	13.20	0.623	0.742	0.257	8.45	27
ZnO:F	0.747	0.889	5.17	2780	12.60	0.596	0.716	0.177	8.37	28
ZnO:F	0.743	0.897	5.31	2830	13.02	0.583	0.707	0.207	8.68	12
ZnO:F	0.744	0.901	5.25	2740	12.36	0.574	0.707	0.185	8.29	18
ZnO:F	0.741	0.895	5.29	2590	12.85	0.608	0.732	0.265	8.52	13
ZnO:F	0.737	0.897	5.55	2480	12.77	0.578	0.709	0.224	8.44	15
Average:										
ZnO:F	**0.734**	**0.881**	**5.69**	**2700**	**12.78**	**0.601**	**0.723**	**0.236**	**8.43**	**19**
SnO_2:F	**0.738**	**0.883**	**5.61**	**2740**	**11.63**	**0.544**	**0.677**	**0.229**	**7.58**	**8**

Figure 7. Graphical Representation of the Solar Cell Parameters Using the BP Solar Buffer Layer.

072301: A Summary of ZnO Front Contact samples
Sample sets received on 5-10-01 and 6-15-01

Oneway Analysis of FF By Process 1

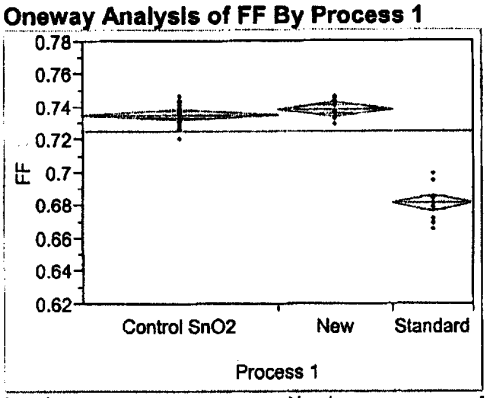

Level	Number	Mean
Control SnO2	22	0.735318
New	13	0.738769
Standard	9	0.681333

Oneway Analysis of Jsc By Process 1

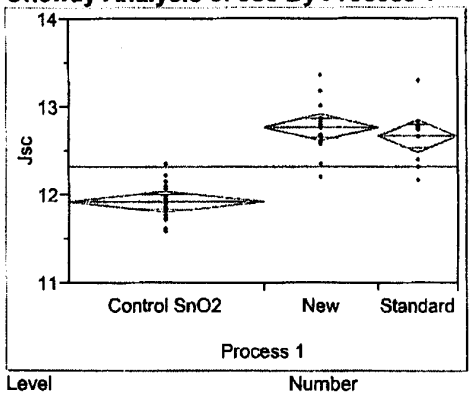

Level	Number	Mean
Control SnO2	22	11.9268
New	13	12.7715
Standard	9	12.6722

Oneway Analysis of Voc By Process 1

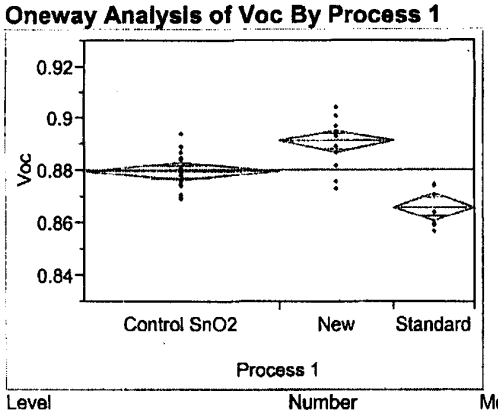

Level	Number	Mean
Control SnO2	22	0.879500
New	13	0.891154
Standard	9	0.866000

Oneway Analysis of Eff By Process 1

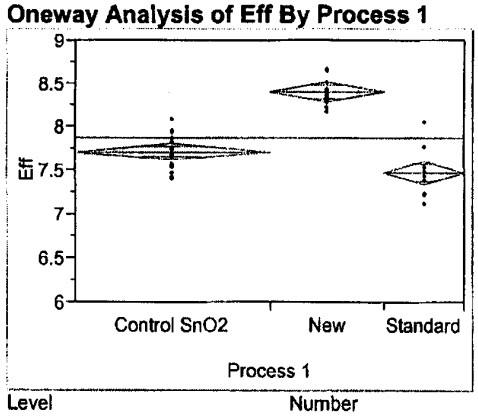

Level	Number	Mean
Control SnO2	22	7.71455
New	13	8.40769
Standard	9	7.47889

Oneway Analysis of Rs By Process 1

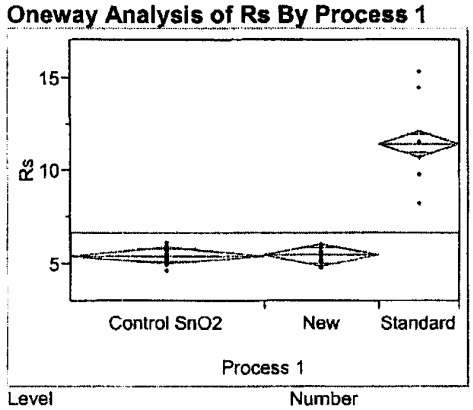

Level	Number	Mean
Control SnO2	22	5.4845
New	13	5.5069
Standard	9	11.4511

Oneway Analysis of Shunts By Process 1

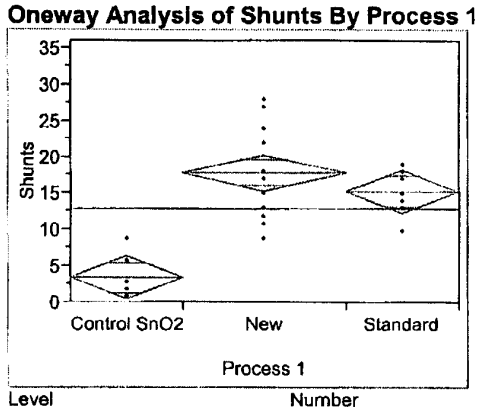

Level	Number	Mean
Control SnO2	9	3.4444
New	13	17.8462
Standard	9	15.3333

Task 2: CVD of Fluorine-Doped Zinc Oxide Films

Zinc acetylacetonate, an inexpensive and commercially available material was used successfully for depositing zinc oxide films. Extensive tests of several fluorine-containing materials as potential fluorine dopants, failed to increase the conductivity of zinc oxide films deposited from zinc acetylacetonate. Thus the tetramethylethylenediamine adduct of diethylzinc along with the effective fluorine dopant benzoyl fluoride, is still the best way to deposit highly conductive and transparent fluorine-doped zinc oxide.[10]

In our first annual report, we showed that etching our ZnO:F samples in hydrochloric acid markedly improved the quality of the solar cells deposited on them. Repeated attempts to reproduce those results have failed. New samples of hydrochloric-acid etched ZnO:F films were sent to BP Solar, where tandem a-Si solar cells were deposited on these superstrates. Each deposition run had side-by side ZnO:F and SnO_2:F (made by AFG) superstrates. The ZnO:F cells showed an average of 7% higher current, because of their higher optical transmission, as well as a 1% higher average open circuit voltage. However, the fill factors of the ZnO:F cell averaged about 6% lower, so the overall efficiencies of the ZnO:F cells were only slightly higher than the SnO_2:F cells. Typical results for two runs are shown in Table 4.

Table 4. Tandem a-Si cell parameters for two runs with side-by side ZnO:F and SnO_2:F superstrates.

	Run #	FF	Voc volts	Rs ohms	Jsc1 ma/cm^2	Jsc2 ma/cm^2	Eff. (%)	Shunts (%)
ZnO:F	1	0.6888	1.515	20.8	8.40	7.89	8.49	58
ZnO:F	1	0.675	1.507	33.02	8.29	8.08	8.33	75
ZnO:F	1	0.679	1.517	27.64	8.26	7.69	8.21	78
ZnO:F	1	0.668	1.516	20.36	8.52	8.91	8.83	92
ZnO:F	2	0.661	1.497	23.16	8.03	8.95	8.40	75
ZnO:F	2						0.00	100
ZnO:F	2	0.667	1.525	28	8.31	8.42	8.51	89
ZnO:F	2						0.00	100
SnO_2:F	1	0.717	1.491	15.5	7.96	7.63	8.33	8
SnO_2:F	1	0.709	1.491	17.22	8.11	7.69	8.35	22
SnO_2:F	1	0.717	1.498	16.49	8.12	7.35	8.31	6
SnO_2:F	1	0.710	1.498	14.72	8.2	7.25	8.22	3
SnO_2:F	2	0.711	1.494	14.99	7.96	7.90	8.42	6
SnO_2:F	2	0.713	1.498	15.37	7.97	7.96	8.51	17
SnO_2:F	2	0.709	1.506	15.52	7.96	7.99	8.52	22
SnO_2:F	2	0.703	1.499	16.3	7.97	8.19	8.51	19

A wide variety of surface treatments were tried in order to improve the fill factors. A set of samples of hydrochloric-acid etched ZnO:F was sent to BP Solar, where single-junction a-Si

solar cells were deposited on these superstrates. The deposition recipes for the p-layer were varied in order to maximize the efficiency of the cells. The result was that the efficiencies were eventually increased to be comparable to the standard cells made on SnO_2. The detailed cell results are summarized in the following Table.

Table 5. Tandem a-Si cell parameters for runs with side-by side ZnO:F and SnO_2:F superstrates.

TCO	Recipe	FF	Voc volts	Rs	Rsh	Jsc	QE 440	QE 500	QE 700	Eff. %	Shunts %
ZnO	Standard	0.656	0.791	6.84	1340	13.02	701	778	226	6.76	78
SnO_2	Single Jun.	0.728	0.899	5.46	3560	11.65	598	693	226	7.62	47
ZnO	µc-p +a-p	0.691	0.882	8.64	1820	11.81	606	717	192	7.20	61
SnO_2		0.719	0.876	5.9	1820	8.89	456	551	134	5.60	53
ZnO	µc-P2 +a-p	0.657	0.848	13.24	2250	12.18	663	754	176	6.79	97
SnO_2		0.753	0.892	5.01	2640	10.73	565	669	171	7.21	42
ZnO	a-p+µcp	0.493	0.516	11.36	2320	10.89	493	605	219	2.77	97
SnO_2		0.545	0.789	8.09	3250	11.07	511	627	231	4.76	47
ZnO	H_2 pl. 100s	0.677	0.894	12.53	2200	12.27	637	748	221	7.43	39
SnO_2	+aP	0.745	0.898	5.51	2620	10.86	535	646	185	7.27	3
ZnO	H_2 pl. 200s	0.713	0.846	5.64	2250	12.64	626	733	237	7.62	53
SnO_2	+a-P	0.727	0.888	5.62	2720	10.34	498	612	177	6.68	6
ZnO	H_2 pl. 200s	0.655	0.875	6.64	1150	12	546	686	248	6.88	75
SnO_2	+ thick a-P	0.693	0.905	5.44	1160	9.96	444	579	178	6.25	14
ZnO	µcP only	shunt									100
SnO_2		shunt									100

The first pair of samples, labeled Standard Single Jun., represent cells grown under conditions optimized for SnO_2 superstrates. The short-circuit current (Jsc) and the quantum efficiencies (QE) are larger for cells on ZnO:F than for the cells on SnO_2:F. This result is expected because of the higher optical transmission of the ZnO:F. Evidently, these conditions are not optimum for electrical contact to the ZnO, since the fill factor and open circuit voltage are lower for cells on ZnO than for those on SnO_2. Hence the efficiency is lower for the ZnO:F cells made under conditions standardized for SnO_2:F.

The next run inserted a micro-crystalline p-layer (μc-p) prior to the usual amorphous p-layer (a-p). This resulted in improving the fill factor, voltage and efficiency of the ZnO:F cells to values close to, but still slightly below, those of the standard cells. A second micro-crystalline recipe (μc-p2) was less successful. Reversing the order of the μc-p and a-p layers produced terrible results, as expected.

The next three runs introduced a hydrogen plasma clean prior to deposition of the standard amorphous p-layer. A 200 second hydrogen plasma clean improved the efficiency of the ZnO:F cells made with the standard recipe up to values equal to those of the standard SnO_2:F cells. The same hydrogen plasma clean significantly degraded the currents of the SnO_2:F cells, probably by causing reduction of the tin oxide and consequent lowering of the optical transmission. As expected, the zinc oxide was not reduced by the plasma clean.

Many solar cells deposited on the ZnO:F superstrates were shunted, while adjacent superstrates of SnO_2:F showed much smaller "normal" numbers of shunts. Table 1 gives some typical results for numbers of shunts. On some ZnO:F samples, all 36 cells were shunted. For example, the final pair of samples in Table 5, made with only a μc-p layer and no a-p layer, were all shunted.

An electron microscopic study of the morphology of the etched zinc oxide samples was undertaken in order to try to identify the reason for the large number of shunts. As a base for comparison, Figure 8 shows a scanning electron microscope (SEM) picture of the normal textured surface of polycrystalline fluorine-doped zinc oxide as deposited by our CVD process. It shows crystallites with their points projecting from the surface. This texture provides excellent light-trapping. Many a-Si solar cells have been grown previously on similarly textured SnO_2:F films without significant shunting problems.

Figure 8. SEM of Fluorine-Doped Zinc Oxide as Deposited.

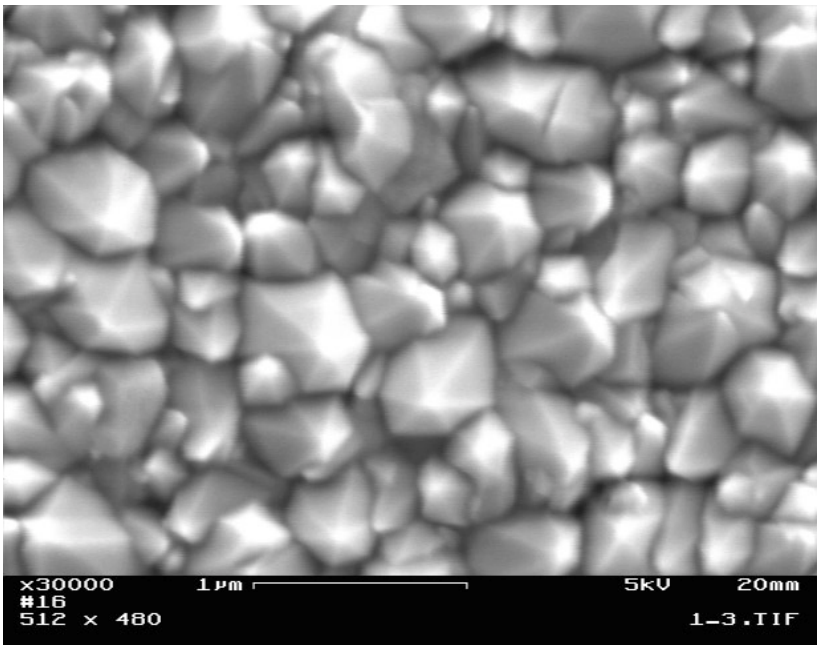

A SEM of a fluorine-doped zinc oxide film etched in hydrochloric acid is shown in Figure 9. It has many deep and narrow etch pits.

Figure 9. SEM of Fluorine-Doped Zinc Oxide after a 30-Second Etch in Dilute (0.1M) Hydrochloric Adcid.

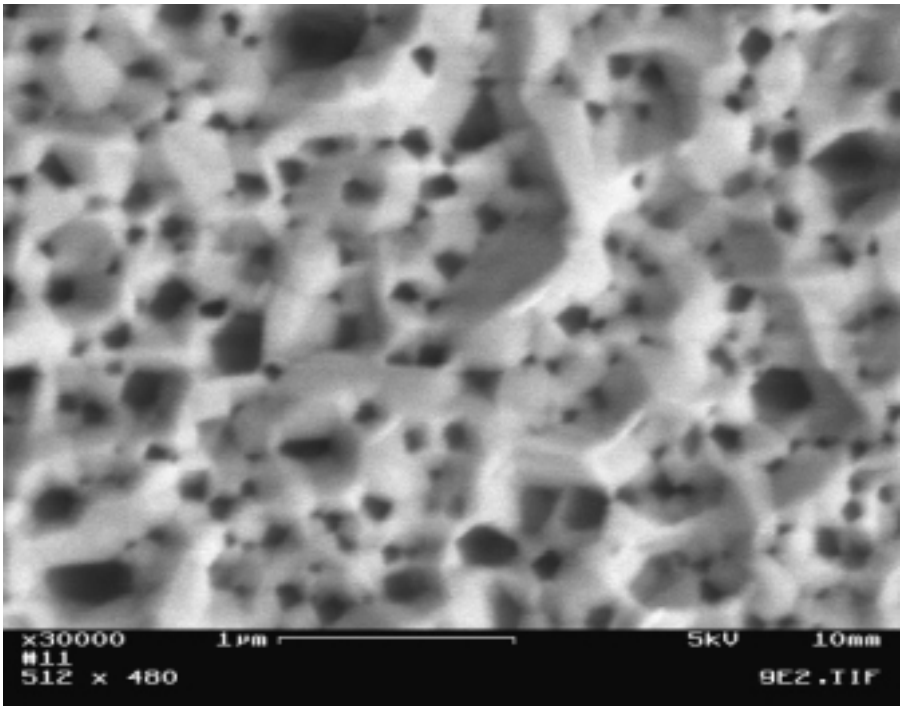

If the step coverage of the amorphous silicon deposition is not good enough, then shunts may be produced through thin areas at these etch pits. However, etch pits cannot account for most of the shunts, since similar numbers of shunts have been found with non-etched ZnO:F superstrates.

Baking the ZnO:F films to remove adsorbed materials, such as water, prior to a-Si deposition did not reduce the number of shunts. Polishing the ZnO:F films with successively finer diamond powders has not reduced the numbers of shunts, either. The origin of the shunts remains a mystery.

Task 3: CVD of Aluminum Oxide Films

Aluminum oxide-coated glass plates are used as substrates for deposition of fluorine-doped zinc oxide for three different reasons:

1) Use of an alumina layer between soda-lime glass and fluorine-doped zinc oxide films was found to provide a 10% reduction in their sheet resistance. Alumina is an outstanding barrier to diffusion of sodium. Thus it prevents contamination of the film by sodium, which traps and scatters the conduction electrons in the zinc oxide films.

2) Nucleation of fluorine-doped zinc oxide appears to be more uniform and consistent on alumina surfaces than on bare glass substrates. Thus it provides better control of roughness

and the resultant haze that is needed for efficient light-trapping in amorphous silicon solar cells.

3) The transmission of light through the films is increased by a per cent or so because alumina has a refractive index intermediate between that of glass and zinc oxide.

Two different liquid precursors were investigated for the CVD of alumina films: triethyldialuminum tri-*sec*-butoxide[1] and mixed aluminum betadiketonates.[2] Both of these precursors are now commercially available from Strem Chemical Company, Newburyport, MA. Both precursors were used successfully to make amorphous aluminum oxide films used in this project.

References

[1] Roy G. Gordon, Keith Kramer and Xinye Liu, Materials Res. Soc. Proc. **446**, 383 (1997); Roy G. Gordon, Keith Kramer and Xinye Liu, US Patent 6,037,003 (2000).
[2] Roy G. Gordon, Feng Chen, Nicholas J. DiCeglie, Jr., Amos Kenigsberg, Xinye Liu, Daniel Teff and John Thornton, Materials Res. Soc. Proc. **495**, 63 (1998); Roy G. Gordon, US Patent 6,258,157 (2001).
[3] R. G. Gordon, J. Proscia, F. B. Ellis, A. E. Delahoy, Solar Energy Materials **18**, 263-281 (1989); J. Proscia, R. G. Gordon, Thin Solid Films **214**, 175-187 (1992).
[4] J. Hu, R. G. Gordon, Solar Cells **30**, 437-450 (1991).
[5] S. Hegedus, H. Liang and R. G. Gordon, Amer. Inst. Phys. Conf. Proc. **353** (13th NREL Photovoltaics Program Review, 1995), 465-72 (1996).
[6] Roy G. Gordon, R. Broomhall-Dillard, X. Liu, D. Pang, J. Barton, Annual Technical Report, NREL Subcontract No. XAK-8-17619-26 (2000)
[7] Zinc stannate buffer layers have recently been reported to increase the efficiency of CdTe superstrate cells: X. Wu, R. Ribelin, R. G. Dhere, D. S. Albin, S. Asher, D. H. Levi, A. Mason, H. R. Moutinho, P. Shelton, Proceedings of the 28th IEEE Photovoltaic Specialists Conference (Anchorage, AK), p. 470 (2000).
[8] Natl. Bur. Stand. (U.S.) Monogr. **25**, 1062 (1972).
[9] Coffeen, J. Am. Ceram. Soc. **36**, 207 (1953).
[10] Roy G. Gordon, Keith Kramer and Haifang Liang, US Patent 6,071,561 (2000).

REPORT DOCUMENTATION PAGE

Form Approved
OMB NO. 0704-0188

1. AGENCY USE ONLY (Leave blank)	2. REPORT DATE	3. REPORT TYPE AND DATES COVERED
	December, 2001	Final Technical Report 15 June 2001

4. TITLE AND SUBTITLE
Transparent Conductors and Barrier Layers for Thin Film Solar Cells, Final Technical Report, 15 June 2001

5. FUNDING NUMBERS
CF: XAK-8-17619-26
PVP25001

6. AUTHOR(S)
R.G. Gordon, R. Broomhall-Dillard, X. Liu, D. Pang, and J. Barton

7. PERFORMING ORGANIZATION NAME(S) AND ADDRESS(ES)
Harvard University
Cambridge, Massachusetts

8. PERFORMING ORGANIZATION REPORT NUMBER

9. SPONSORING/MONITORING AGENCY NAME(S) AND ADDRESS(ES)
National Renewable Energy Laboratory
1617 Cole Blvd.
Golden, CO 80401-3393

10. SPONSORING/MONITORING AGENCY REPORT NUMBER
NREL/SR-520-31379

11. SUPPLEMENTARY NOTES
NREL Technical Monitor: Bolko von Roedern

12a. DISTRIBUTION/AVAILABILITY STATEMENT
National Technical Information Service
U.S. Department of Commerce
5285 Port Royal Road
Springfield, VA 22161

12b. DISTRIBUTION CODE

13. ABSTRACT *(Maximum 200 words)* This report describes the research undertaken to increase the efficiency of thin-film solar cells based on amorphous silicon in the so-called “superstrate structure” (glass front surface/transparent electrically conductive oxide (TCO)/pin amorphous silicon/metal back electrode). The TCO layer must meet many requirements: high optical transparency in the wavelength region from about 350 to 900 nm, low electrical sheet resistance, stability during handling and deposition of the subsequent layers and during use, a textured (rough) surface to enhance optical absorption of red and near-infrared light, and low-resistance electrical contact to the amorphous silicon p-layer. Fluorine-doped tin oxide has been the TCO used in most commercial superstrate amorphous silicon cells. Fluorine-doped zinc oxide (ZnO:F) was later shown to be even more transparent than fluorine-doped tin oxide, as well as being more resistant to the strongly reducing conditions encountered during the deposition of amorphous silicon. Solar cells based on ZnO:F showed the expected higher currents, but the fill factors were lower than standard cells grown on tin oxide, resulting in no consistent improvement in efficiency. This problem was recently mitigated by using a new proprietary p/buffer layer combination developed at BP Solar.

14. SUBJECT TERMS PV; thin-film solar cells; superstrate structure; transparent conductive oxide (TCO); fluorine-doped; proprietary buffer layer; shunted cells; precursors; haze and light trapping

15. NUMBER OF PAGES

16. PRICE CODE

17. SECURITY CLASSIFICATION OF REPORT	18. SECURITY CLASSIFICATION OF THIS PAGE	19. SECURITY CLASSIFICATION OF ABSTRACT	20. LIMITATION OF ABSTRACT
Unclassified	Unclassified	Unclassified	UL